Seagrass Meadow Mapping in the Bay of Bengal Using Machine Learning and Remote Sensing

Lingeswaran A[1], Melvin Fredrick J S[1], Lathaselvi G[2], Vimalathitthan Shanmugam[3*]

[1]Student, Department of Information Technology,

St. Joseph's College of Engineering, Chennai, India

[2]Associate Professor, Department of Information Technology,

St. Joseph's College of Engineering, Chennai, India

[3]Assistant Professor, Department of Information Technology,

St. Joseph's College of Engineering, Chennai, India

*vimalathitthan@stjosephs.ac.in

Abstract : Seagrass meadows play a crucial role in maintaining coastal biodiversity, stabilizing sediments, and mitigating climate change through carbon storage, yet they are declining rapidly due to human-induced pressures. Effective large-scale monitoring remains difficult, particularly in turbid coastal waters where field-based surveys are limited. This study presents a satellite-based framework for mapping seagrass distribution using multispectral imagery from Sentinel-2. The input data were corrected, normalized using Min-Max scaling, and resampled to a uniform 10-m spatial resolution. Spectral reflectance patterns and vegetation indices were employed to distinguish seagrass from surrounding benthic features, and the classification process was validated against reference observations. The mapping workflow was applied using a chunk-based approach to handle large raster datasets efficiently, generating probability surfaces and binary presence–absence maps of seagrass cover. The results demonstrate high thematic accuracy and clear spatial delineation of seagrass habitats, even under challenging water conditions. This framework offers a reproducible and cost-effective tool for long-term ecological monitoring, providing critical information for conservation planning, restoration initiatives, and sustainable management of coastal ecosystems.

Keywords: *Seagrass, Random Forest, Sentinel 2 L2A, Resampling, Bay of Bengal*

Introduction

Seagrass beds are keystone components of coastal ecosystems delivering crucial services such as storing carbon, providing nursery habitat for important fish, stabilizing sediments, and coastal defence (Hossain et al., 2015). Despite being highly valuable to their ecological as well as socio-economic roles, seagrass communities undergo a global decline owing to coastal land use alterations, pollution, over-fishing, and climate-driven changes (Hossain et al., 2015). Additional studies emphasize that seagrass loss is accelerating in many tropical regions due to cumulative anthropogenic stressors, highlighting the need for scalable monitoring frameworks (Pasqualini et al., 2001). The Gulf of Mannar and its vicinal Palk

Bay, the coastline between southeastern India to northwestern Sri Lanka's coastline, is a hotbed of sea biodiversity as well as coastal livelihoods but is challenging to observe at a large scale owing to shallowness of bathymetry, complex island reef geometry, variable water optical properties, as well as occasional turbidity (Geevarghese et al., 2018; Govindasamy et al., 2013; Maheswari, 2013; Paulose et al., 2013; Roelfsema et al., 2014). To compensate for variable native spatial resolution between bands selected, some bands being represented at 20 m resolution with others represented at 10 m resolution, 20 m bands are down-sampled to 10 m resolution as part of a preprocessing to yield harmonized inputs amenable to pixelwise classification (Pu et al., 2012). We create our training data from labelled spectral datasets accompanying paired field-confirmed observations and reference maps with extracted band values (Komatsu et al., 2020; Roelfsema et al., 2009, 2016; Strydom et al., 2021; Vahtmäe et al., 2024). Choice of Random Forest algorithm to classification because it is robust to noisy features, can handle non-linear class boundaries, and has intrinsic feature-importance metrics to enable interpretability within a multispectral framework (Effrosynidis et al., 2018; Ha et al., 2020). Beyond Random Forest, alternative ensemble methods and hybrid classifiers have also been trailed for seagrass mapping, though their scalability remains debated (Kaufman & Bell, 2022). Model parameters learned and scaling transforms for features are stored to disk to enable reproducible inference over time and across scenes (Ha et al., 2020). Our inference engine is optimized for large-area deployment: satellite scenes are consumed in memory-efficient data chunks, where pixel-vector scaling and classification is applied to produce binary labels (0 = non-seagrass, 1 = seagrass). Classification results are represented as a collection of grayscale maps where black is non-seagrass, white is seagrass, and variable intermediate-grayscale areas indicate ambiguous or areas with potential seagrass that would warrant targeted field validation (Komatsu et al., 2020).

Key contributions of our paper are: (1) an end-to-end scalable pipeline to synchronize multispectral bands with chunked inference for massive coastal scenes; (2) empirical demonstration of Random Forest efficacy on an 8-band spectral data set for delineation of submerged vegetation across the Gulf of Mannar / Palk Bay; and (3) functional seagrass maps to inform conservation priority planning, fishery management decisions, and restoration planning across an area with high ecological as well as human dependence. We also note limitations according to water-column variation, impacts from mixed pixels about complex reef and island structures, and future additions such as time-series change

detection, quantification of uncertainty for suspicious zones, as well as successive refinement of our models through integration with concentrated in-situ surveys (Carter et al., 2021; Komatsu et al., 2020; Lyons et al., 2013; Phiri et al., 2020; Roelfsema et al., 2009). The remainder of our paper details data sources, pre-processing steps, development of our models including choice among multiple alternatives, results from our validations, as well as coastal management applications.

Literature Review

Seagrass meadows yield disproportionate socio-economic and ecological services but decline across the globe, creating an imperative for consistent, scalable monitoring (Hossain et al., 2015). Broad-scale seagrass mapping by remote sensing is most feasible economically because extensive coastlines can be mapped repeatedly with remote sensing, but it relies heavily on choice of sensor, preprocessing to remove water-column effects, and successful classification protocols (Komatsu et al., 2020; Phinn et al., 2008).

Basic work emphasizes that identification of seagrass is concerned with discerning subtle spectral variation governed by pigment and canopy geometry. In-situ hyperspectral explorations also indicate that density classes and species should be discernible by reflective attributes within the visible–red edge part but spectral distinctiveness is sometimes overlain by water depth, turbidity, and ground heterogeneity (Fyfe, 2003; Kovacs et al., 2018). Survey-based reviews and practical applications therefore recommend cautionary preprocessing (correcting for the atmosphere, conversion to bottom reflectance, and depth-invariant water-column compensation such as depth-invariant indices) and integration of surveying into the field to train/validation (Hossain et al., 2015; Komatsu et al., 2020; O'Neill et al., 2011). Recent methodological advances also recommend integrating radiative transfer modelling to better correct depth and water-column variability, which has shown improved results for benthic vegetation mapping (Koedsin et al., 2016). Sensor comparisons point to trade-offs among spatial, spectral, and temporal resolution. (Phinn et al., 2008) and (Kovacs et al., 2018) indicate that hyperspectral or very-high-resolution imagery has stronger coverage of fine details on the seabed and patchy beds than multispectral sensors with medium resolution but that Sentinel-2 and Landsat remain viable for area coverage where revisit is a concern or expense is an issue. Other comparative work suggests that integrating Landsat time-series with Sentinel imagery can offer complementary temporal

insights while maintaining continuity with historical baselines (Parthasarathy et al., 1991). Accordingly, operational workflows typically combine multispectral bands (e.g., Sentinel bands B2–B8A) and down sample bands to a standard spatial scale to ensure a maximum amount of informative data is available throughout the scene (McKenzie et al., 2022; Pu et al., 2012).

Methodologically, we've witnessed a clear shift from statistical-classifier-based to machine-learning- and deep-learning-based classification. There's been a tendency toward ensemble strategies particularly Random Forest since they handle noisy multispectral features, avoid overfitting with sparse labelling data, and provide feature-importance diagnostics (Effrosynidis et al., 2018; Ha et al., 2020). Beyond Random Forest, alternative ensemble methods and hybrid classifiers have also been trailed for seagrass mapping, though their scalability remains debated (Kaufman & Bell, 2022). It's been discovered by comparative studies that Random Forest and several ensembles approach overwhelmingly succeed maximum-likelihood classification on Sentinel-2 data, though CNNs offer hope where very-high-resolution imagery and dense labels for learning can be found (Ha et al., 2020; Mohamed et al., 2020). There is also increasing attention on semi-supervised and transfer learning approaches, which can leverage limited field data to improve classifier robustness across new coastal regions (Islam, 2021). Region-specific Indian surveys indicate promise alongside challenges for applied mapping off Palk Bay/Gulf of Mannar. Country-scale and region-based syntheses indicate broad coverage by seagrass off south-eastern Indian shores and document spatial–temporal changes governed by disturbances and seasonality(Geevarghese et al., 2018; Govindasamy et al., 2013; Paulose et al., 2013). High-resolution sensor applications (e.g., WorldView-2) off Palk Bay indicate advantages of high spatial resolution for patchy habitats conservation (Maheswari, 2013; Roelfsema et al., 2014). Of particular interest, syntheses of long-term monitoring data indicate that integration with satellite time-series is necessary to establish trends to guide management (Carter et al., 2021; Lyons et al., 2013). In combination, the literature facilitates an operational, repeatable pipeline that: (1) uses a selected spectral subset (red-edge visible or beyond), (2) uses strict water-column and spatial harmonization, and (3) uses ensemble classifiers such as Random Forest for pixelwise mapping all supported by field validation and, where available, time-series analysis. These conclusions directly inform our approach to seagrass mapping throughout the Gulf of Mannar / Palk Bay using Sentinel-based bands (B2–B8A), bands

being up sampled or down sampled to a consistent spatial resolution to match repeatedly collected Sentinel imagery via Random Forest classification to produce operational, high-resolution distribution maps for management and conservation.

Methodology

The methodology in this work is designed to capture key specific area and modules of the process flow. Figure 1 shows us that each module is as important steps to take precise steps for implementing the model that gives us a better result in terms of accuracy and seagrass mapping over a specific area of interest**.**

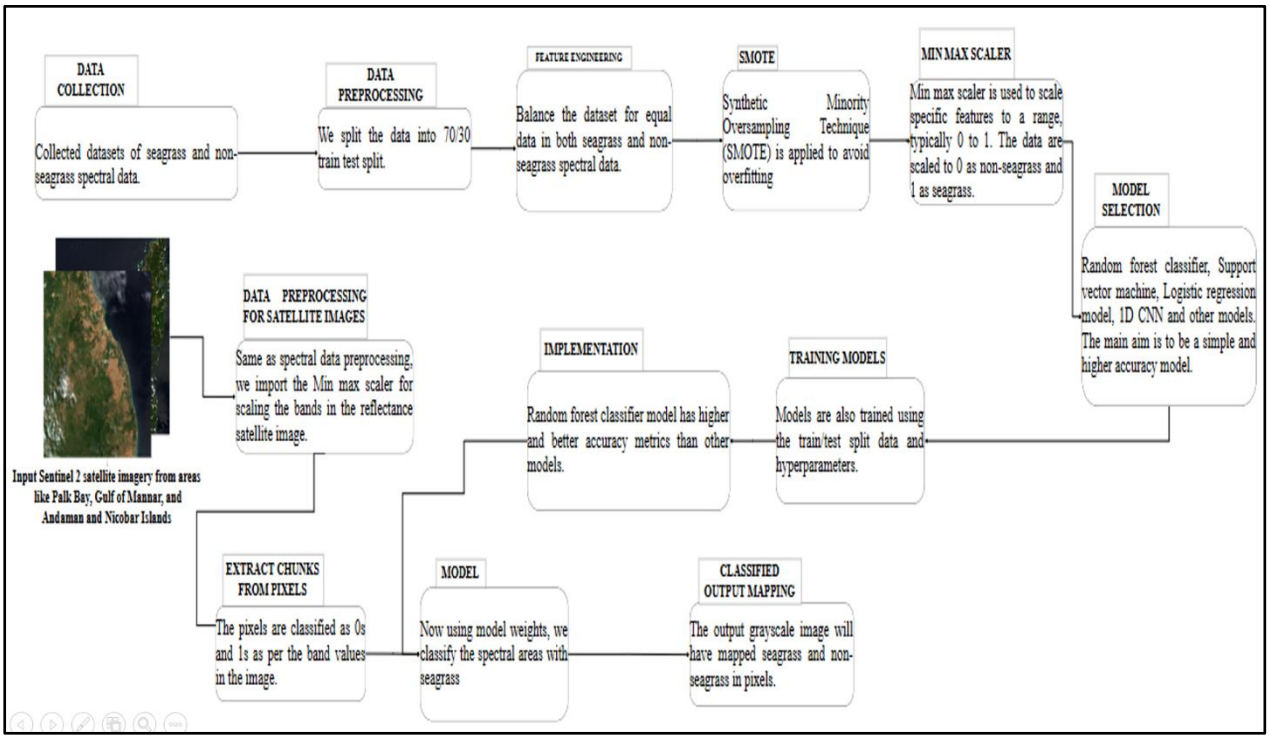

Figure 1. Complete Model Architecture diagram with modules. Each explaining the steps and process flow of the implementation of the proposed model

Data Collection

We collected data from complementary satellite products, global occurrence datasets, regional boundary files, and released spectral libraries to generate a comprehensive reference database for seagrass pixels to map. Sentinel-2 Level-2A surface-reflectance composites were used as imagery with high preference because they present 10 m spatial

resolution for visible and near-infrared bands that is ideal for detection of vegetation occurring in shallows water. Figure 2 shows are the area of interest in our research work over Bay of Bengal. The AOI in our work covers Palk Bay, Gulf of Mannar, and Andaman and Nicobar Islands over the Bay of Bengal region. Global distribution and occurrence layers for seagrasses were used to identify established locations of their habitat and to guide selection of exemplary locations for study and validation samples. Country-level administrative shapefiles were used to clip Sentinel-2 imagery to coastal region of interest and to enable stratified sampling within nation-state borders. Published spectral reflectance compilations for seagrasses, algae, submerged aquatic vegetation, and common types of substrates were used to generate a spectral reference library and to guide anticipated spectral behavior and mixed-pixel behavior occurring shoreward. A global database of seagrass structural attributes (e.g., canopy height, density, biomass surrogates) were also consulted to enable subsequent validation for mapped cover. All datasets were also annotated with metadata regarding spatial resolution, acquisition date, and origin to enable reproducibility and to enable subsequent harmonizing throughout subsequent preprocessing steps and data analysis. Sources include Sentinel-2 Level-2A repositories, international seagrass distribution data compilations, nation-state repositories for shapefiles, and peer-reviewed/archival spectral and ecological data compilations.

Figure 2. Location map of the area of interest that we are focusing i.e. (Palk Bay, Gulf of Mannar, and Andaman and Nicobar Islands) in the Bay of Bengal

classification input. Sentinel-2 Level-2A scenes were trimmed to our area of investigation and clouds were filtered out using SCL (Scene Classification Layer) and ancillary clouds masks. Saturated pixels as well as clouds were also filtered out. Bands from B02 to B8A (inclusive) including blue, green, red, red-edge and near-infrared bands were selected; bands provided with coarser native scales were bilinearly downscaled to 10 m and were registered to a common grid. Ancillary layers (administrative masks, spectral library-based endmembers, and structural seagrass variables) were appended where needed. Outlier pixels with extreme reflectance levels were discovered and removed through percentile clipping and lower/upper sensor-knowledge-based bounds. Stratified pixel samples were taken to create train, validate and test sets to prepare data for machine learning; an imbalance between classes discovered within the train set was adjusted for by utilizing SMOTE (Synthetic Minority Over-sampling Technique) to create minority-class (seagrass) samples synthetically with original distribution remaining intact for validate and test sets. A Min–Max scaler was trained to the train features and then applied throughout portions to scale inputs into the [0,1] range. Finally, a preprocessing pipeline, scaler parameters, and sampling logs were versioned to allow for reproducibility and same transformations upon deployment for inferencing with a model.

(a)

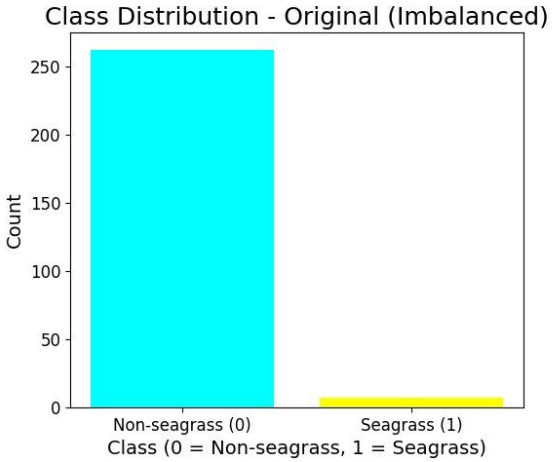

Figure 3(a) This figure represents the original class distribution from the datasets that we acquired. As we can see they are highly imbalanced.

(b)

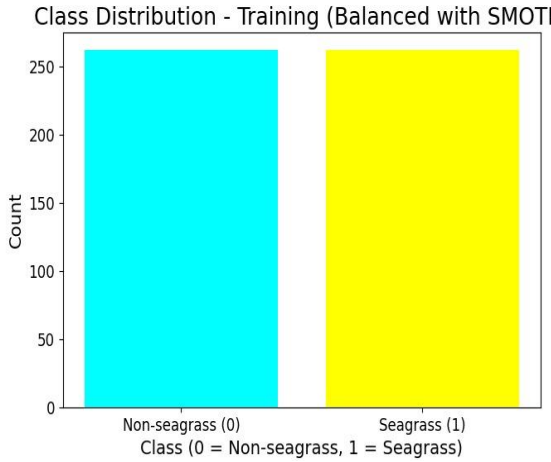

Figure 3(b) This is the balanced class distribution between seagrass and non-seagrass using SMOTE. Here seagrass is classified as 1 and non-seagrass as 0

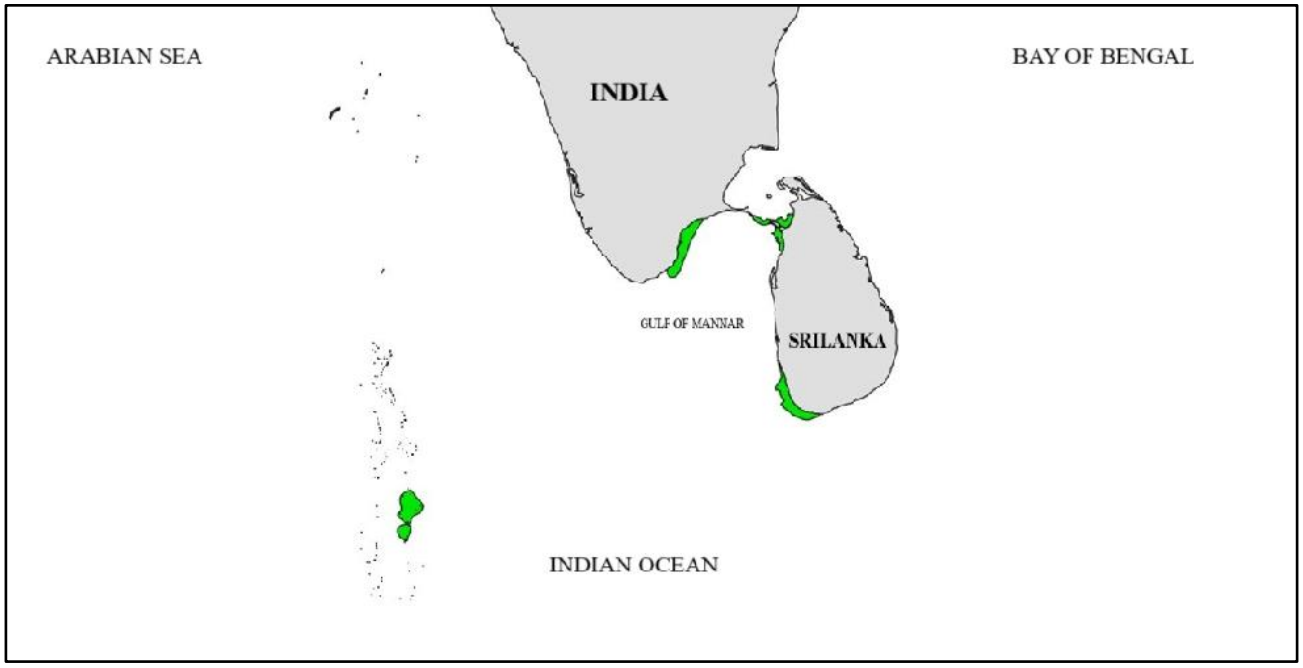

Figure 5. This figure shows us the potential areas of the seagrass that are present over the coastal lines of India and Sri Lanka. The seagrass typically grows around the coastal shores of the country.

Feature Engineering

SMOTE is generally used for balancing the datasets that are imbalanced in any form. The main reason for making the datasets balanced is to ensure the risk of overfitting in the model architecture. If in any way, we train the model with an imbalanced dataset then, the model tends to be biased on the majority label. It will corrupt the model purpose and cannot be able to identify the other labels and classes across the datasets. Figure 3a shows us the imbalanced class distribution obtained from different datasets as spectral data for seagrass and non-seagrass. Figure 3b shows us the balanced class distribution dataset after applying SMOTE to the spectral data. With this, we have avoided overfitting our data into the model. Preprocessing by feature engineering served to transform preprocessed spectral data and into a structured classification space for a supervised classification. Sentinel-2 Level-2A imagery was standardized first to a single 10 m resolution to ensure that all spectral bands from Sentinel-2's B02 (blue) to Sentinel-2's B8A (near-infrared and red-edge bands) were spatially registered. Bands originally produced with finer resolution were down-sampled with bilinear interpolation and co-registered to a standard grid to allow pixel-level comparisons throughout the visible, red-edge, and near-infrared spectrum.

$$\boldsymbol{xnew = xi + \delta \cdot (xzi - xi)} \quad (1)$$

In addition to raw reflectance data, computable spectral indices were incorporated as engineered features to ensure maximum class separability among submerged vegetation, unvegetated substrate, and water. Library spectra for seagrass as well as algal flora were compared to identify diagnostic wavelengths, which were then used to design customized band ratios tailored to aquatic plants. 1 nm spectral resolution library datasets were binned collectively to match Sentinel-2's discrete multispectral mode setting to generate an equivalent feature set for learning. All value features were also Min–Max scaled with a constraint to be between 0 and 1 by using the formula presented in (2) to prevent higher-magnitude bands' domination and enable each spectral variable to contribute proportionally to the classifier. Final engineered feature set combined resampled reflectance data with vegetation indices and Min–Max-normalized spectral descriptors into a standard input matrix. It was formulated to maximize discriminatory power with retention of physical interpretability of features to be exploited by subsequent machine learning and ecological validation.

$$\boldsymbol{xscaled = x - xmin \,/\, xmax - xmin} \quad (2)$$

Figure 6. These are the sentinel 2 satellite images that we will be using to train the model. We extract the bands from the images ranging from B2 to B8A bands.

Model Selection

The input images of the AOI that we have obtained from the sentinel 2 satellite image are extracted as bands ranging from B2 to B8A. These bands are specifically chosen so that the spectral data can be obtained by the satellite sensors. Typically, as per research, the seagrass reflects sunlight off the surface of water and it is captured by the satellite sensors. Figure 6 shows us the input images that are taken of AOI and the resolution are rescaled to 10m for spatial mapping of the seagrass. It was selected for pixel-level seagrass mapping because Random Forest has a superb trade-off between predictive power, interpretability, and usability for operational application. It is an ensemble decision tree that is capable of dealing with high-dimensional spaces i.e., a number of spectral bands, calculated bands, and ancillary data without extensive feature simplification. It has capability to represent complex, non-linear information with a good match to non-linear spectral mixing and variable water-column effects that are common to coastal aquatic environments. Random Forest is insensitive to noisy and partially incorrect data, a strength for processing multi-source data with changing atmospheric or water conditions. The algorithm produces calibrated class-probability estimates that enable decision thresholds (e.g., a 0.7 probability threshold) to be placed to balance precision versus recall for conservative seagrass detection. Intrinsic mechanisms such as out-of-bag error estimation and tree-ensemble averaging reduce overfitting risk and enable validation. Practicalities also prompted this choice: Random Forest has relatively low hyperparameter tuning compared to most machine-learning alternatives, parallelizes straightforwardly for high pixel amounts, and accepts straightforward model serialization to enable deployment. Note especially that feature-importance measures (Gini or permutation importance) yield interpretable diagnostics that allow tracing decisions to specific bands or indices, facilitating ecological interpretation as well as quality assurance. Even though deep-learning models can be more accurate in specific cases, Random Forest's interpretability, efficiency, and robustness recommend it as a practical solution to the scale of the present study, available labelled data, and purposes of validation.

Training then followed a reproducible, evaluation-based workflow to produce a deployable classifier with traceable artifacts. All labeled data were stratified and split (70% train/30% test) to ensure class ratios were maintained. SMOTE then synoptically balanced the train partition to add minority-class (seagrass) observations with slight majority-class (waterbed) additions while retaining overall class-ratio integrity across splits. A feature-scaling

transform then was fit to train data with subsequent application to all splits to avoid information leakage; fitted scaler then was serialized to be equivalent to preprocessing done during inference. Figure 7 gives us a more refined visualization about the discussion we had in the model selection. We can clearly see the reason why we chose the band values from 2 to 8A. The seagrass reflects off even NIR rays or Near Infrared rays which water absorbs. Therefore, we can differentiate the reflectance values based of the data collected by the satellite sensors.

Training Models

A class weight balanced Random Forest classifier was optimized with a randomized hyperparameter search (numbers of trees, maximum depth, min. samples for split/leaf, and feature sampling schemes) with 3-fold cross-validation and F1 scoring to choose a reliable estimator. Out-of-bag estimates with cross-validation performance were utilized to choose models to guard against overfitting. Probabilistic outputs were saved and investigated with a precision–recall curve to assist with an operational decision threshold; a conservative cutoff (e.g., 0.7) would be selected to maximize precision over recall if false positives are costly. Model evaluation on stored test set included accuracy, precision, recall, F1-score, and a confusion matrix; graphs of precision–recall vs. threshold were produced to allow visualization of trade-offs. End products trained model, scaler, and feature-order list (stored explicitly) were pickled with joblib (rf_model.joblib, scaler.joblib, feature_order.joblib) and results of evaluation (metrics text, image of confusion matrix, graph of precision–recall) were stored to enable reproducibility, deployment, and transparent threshold selection.

Implementation

It is developed to deploy trained Random Forest classification to unseen Sentinel-2 Level-2A imagery for seagrass habitat detection. It is initialized with a subset of eight most relevant spectral bands that were needed for aquatic vegetation surveying: B02 (Blue), B03 (Green), B04 (Red), B05, B06, B07 (Red-edge), B08 (Near Infrared), and B8A (Narrow NIR). These bands were discovered to be automatically found within Sentinel-2 SAFE directory hierarchy such that various acquisition dates as well as granules were versatile to be accepted by the pipeline. Since Sentinel-2 bands were returned with varying spatial scales (10 m, 20 m, 60 m), if a resolution of a band happened to be a coarser version, then it is down-sampled to a 10 m reference grid with bilinear interpolation such that spectral layers would be spatially aligned as well as consistent.

As Sentinel-2 scenes are very large, processing entire scenes directly would be computationally intensive. In order to counter such a challenge, a chunked inference approach was utilized. Imagery was divided into sensible-sized chunks that were read into memory one after another. For each piece or block, pixel data from eight bands selected were extracted and molded into multidimensional feature arrays. These raw digital number measurements were converted to surface reflectance using a scaling factor of 0.0001, as prescribed by Sentinel-2 Level-2A product requirements. Pixel locations with invalid data (e.g., with zeros only) were discarded and eliminated from subsequent prediction steps to avoid classification errors. Every block after processing was passed to the pre-trained Random Forest that was serialized prior to Job lib format. Pre-trained Random Forest generated, for each valid pixel, a probability value representing a probability for presence of seagrass. For interpreting such continuous results into usable maps, a decision threshold value of 0.7 was applied. Pixels having probabilities more than or equal to such a threshold were labeled as seagrass, with others being non-seagrass. Invalid or masked pixels were labeled with a particular no data value of 255 to preserve spatial integrity. Final outputs consisted of two associated raster products. The first one contained a continuous probability raster (seagrass_probability.tif), maintained in 32-bit float format, showing spatial seagrass probability gradients. It was accompanied by a second one containing a discrete classification raster (seagrass_class.tif), encoded as 8-bit integers with associated binary labels and with explicit coding for no data. Both output products retained spatial resolution, coordinate reference system, and georeferencing properties from imagery inputs to enable direct usability within GIS software to view data, add ancillary data coverage overlays, and perform numerical habitat assessments. It is a scalable, reproducible, and environmentally relevant framework for systematic inference that is thus perfect for coastal ecosystem monitoring and long-term conservation planning.

Results and Discussion

Random Forest classifier trained with n_estimators=200, min_samples_split=10, min_samples_leaf=1, max_features='log2', max_depth=None performed sturdyly with respect to held-back test data. On an overall scale, accuracy was 0.9852 with class-specific precision and recall about 0.99 for non-seagrass and about 0.98 for seagrass. At threshold 0.5, only a single error among 135 samples occurred: one non-seagrass pixel classed as seagrass and a seagrass pixel classed as non-seagrass. Classification report thereby suggests a balanced macro

F1 value about 0.98, indicative that discriminator mostly differentiates between both classes under conditions represented within test data. At a scene scale, pipeline produced two principal results: a continuous per-pixel probability raster as a continuous probability map to predict presence of seagrass and a binary classification map. Inferred grayscale image map of region indicates consistent high-probability patches near sheltered shorelines and near isle/reef features with darker shading off shore where cover is unlikely with mid-gray where cover is doubtful.

Model performance and interpretation

In operational terms, interpreting these results, it is reassuring that the model has a very low false positive and false negative count on the test set: false alarms are rare and true seagrass beds are almost never missed on the validation set. The ensemble parameters chosen (moderately large trees, max_features='log2', and conservative splitting) appeared to reduce variance without prescribing overfitting, which aligns with high out-of-sample ability. Persistent final artifacts (rf_model.joblib, scaler.joblib, and feature_order.joblib) ensures that same decision justification and scaling is applied at deployment time, which is critical to reproducibility if one is to process several scenes or repeatedly monitor an area over time. Spatially, the probability raster displays expected ecological patterns: brighter continuous patches reflect shallow sheltered nearshore locations and fringing reef lagoons where seagrass is known to occur. However, the maps display speckle and diffuse bright pixels near complex reef margins and off scape patches. These doubtful signals most likely arise from mixed-pixel effects, submerged substrates with spectral similarity to seagrass (some algae or sand with biofilm), and water optics variation (depth, turbidity, sun-glint). These mid-gray areas also should be taken to represent locations with higher uncertainty than proven presence, and they would be ideal candidates for concentrated field validation before management decisions. From an application perspective, thresholding is a key control point. While the quoted confusion matrix uses a 0.5 decision threshold to enable simplification, practical implementations may choose a slightly higher cutoff (we attempted 0.7) to reduce false positives where verification budgets in the field are restricted. It trades off some recall to gain higher precision and should be selected with consideration to stakeholder priority. Pragmatic post-processing such as morphological filtering or elimination of small objects can effectively reduce lone speckle but preserve higher contiguous beds relevant to ecology.

Conclusion and Recommendation

In this paper we developed and tested an end-to-end pipeline for seagrass mapping across the Gulf of Mannar / Palk Bay with Sentinel-2 spectral bands (B2–B8A), band harmonization (resampling 20 m bands to 10 m), feature engineering, and a Random Forest decision algorithm. On a held-back testing set our model performed exceptionally well (accuracy ≈ 0.99, macro F1 ≈ 0.98), with only two classification errors among 135 samples (one false positive, one false negative at threshold 0.5). Table1 shows us the accuracy results that we have trained among various models. As per the training process, we have selected random forest classifier model as our proposed model due to better results and accuracy. Scene-level results, a continuous probability raster and a classification binary raster produced spatially consistent patterns consistent with ecological expectations: bright, contiguous patches in sheltered nearshore areas and around reef/island features, and dark offshore areas where seagrass is unlikely. In combination, results verify that (1) a properly selected multispectral subset with sensible preprocessing yields highly discriminative input for veg mapping of submerged areas; (2) Random Forest ensembles constitute an effective, interpretable, deployable classifier for such an application; and (3) chunked inference and cached model artifacts make the workflow repeatable and practicable for processing large coastal scenes. In parallel, ambiguous mid-gray areas within probability maps and speckle around complex reef boundaries indicate limitations introduced by mixed pixels, water-column variation, and sensor resolution attributes that require cautious interpretation with subsequent verification.

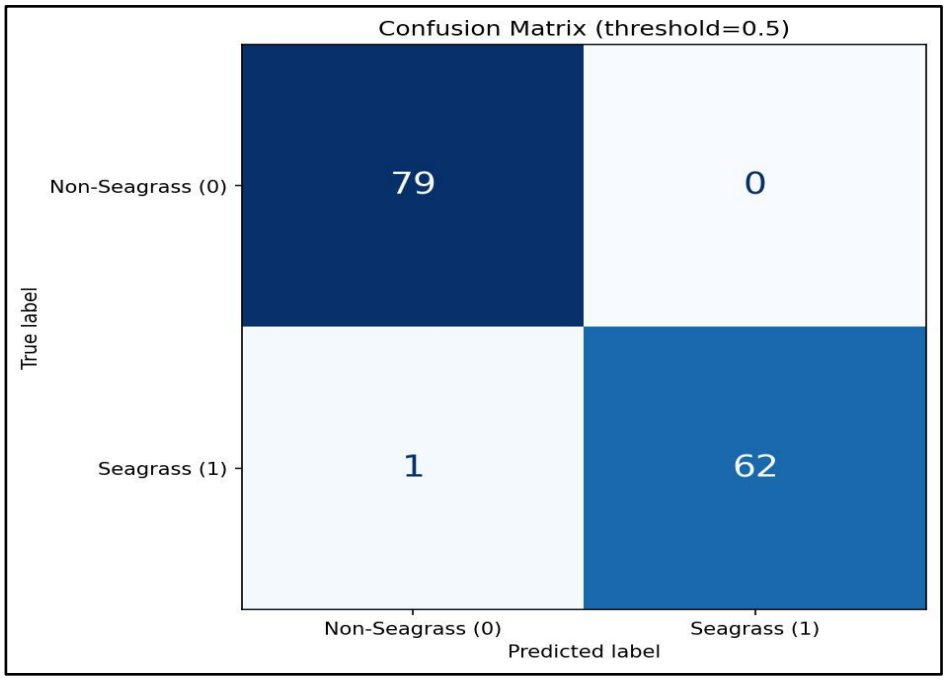

Figure 8. Confusion matrix of the random forest model classifier. Here, we can see non-seagrass and seagrass are both classified with accurate results.

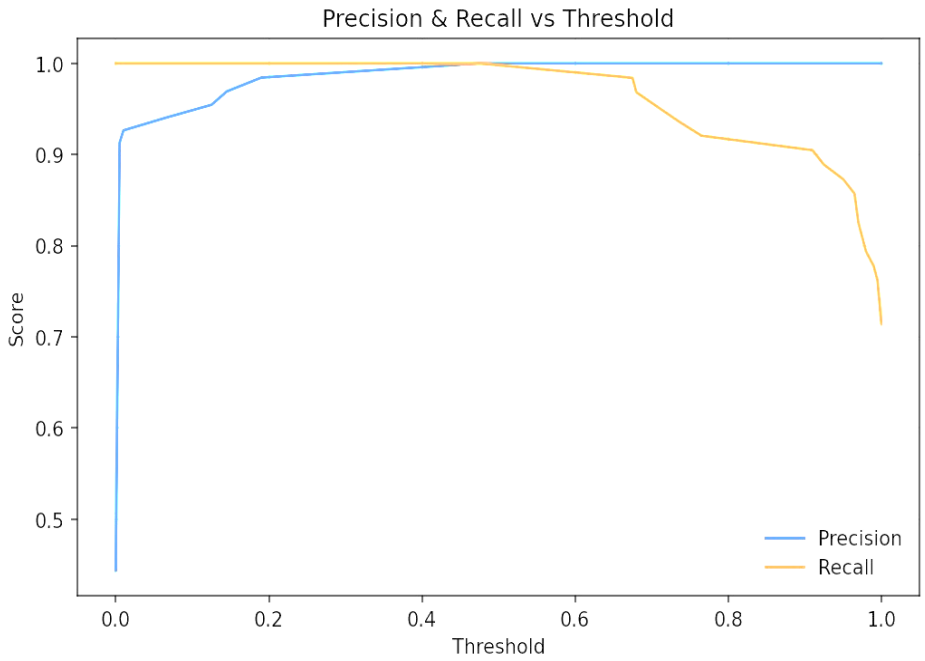

Figure 9. Precision and Recall Graph of the random forest classifier model. This shows us as with the threshold set correctly, we can obtain accurate results.

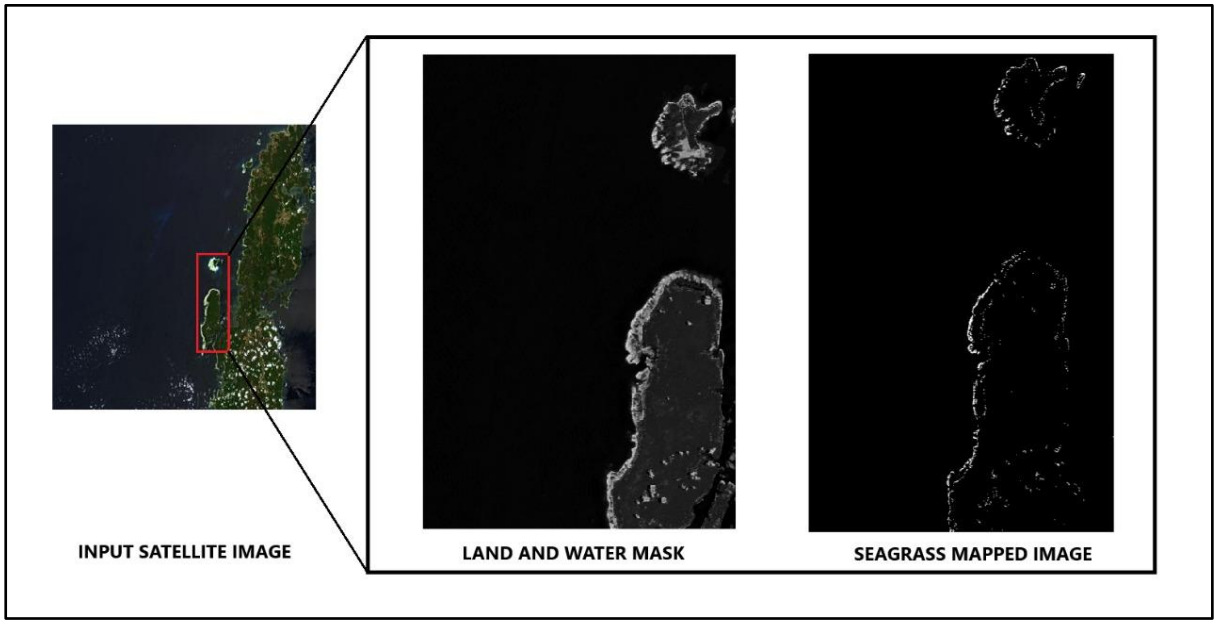

Figure 10. Input images and the corresponding output image with seagrass mapping in grayscale images. The white patches represent the seagrass that are actively mapped.

Table 1. Various proposed models that we have trained and chosen the random forest due to better results in accuracy.

Model	Accuracy	Precision	F1-Score
Random Forest (Proposed Model)	0.99	0.99	0.98
Support Vector Machine	0.93	0.91	0.91
Logistic Regression	0.89	0.86	0.85

References

1. Carter, A. B., McKenna, S. A., Rasheed, M. A., Collier, C., McKenzie, L., Pitcher, R., & Coles, R. (2021). Synthesizing 35 years of seagrass spatial data from the Great barrier reef world heritage area, Queensland, Australia. *Limnology and Oceanography Letters*, *6*(4), 216–226.
2. Effrosynidis, D., Arampatzis, A., & Sylaios, G. (2018). Seagrass detection in the Mediterranean: A supervised learning approach. *Ecological Informatics*, *48*, 158–170.
3. Fyfe, S. K. (2003). Spatial and temporal variation in spectral reflectance: Are seagrass species spectrally distinct? *Limnology and Oceanography*, *48*(1part2), 464–479.
4. Geevarghese, G. A., Akhil, B., Magesh, G., Krishnan, P., Purvaja, R., & Ramesh, R. (2018). A comprehensive geospatial assessment of seagrass distribution in India. *Ocean & Coastal Management*, *159*, 16–25.
5. Govindasamy, C., Arulpriya, M., Anantharaj, K., Ruban, P., & Srinivasan, R. (2013). Seasonal variations in seagrass biomass and productivity in Palk Bay, Bay of Bengal, India. *Int. J. Biodivers. Conserv*, *5*(7), 408–417.
6. Ha, N. T., Manley-Harris, M., Pham, T. D., & Hawes, I. (2020). A comparative assessment of ensemble-based machine learning and maximum likelihood methods for mapping seagrass using Sentinel-2 imagery in Tauranga Harbor, New Zealand. *Remote Sensing*, *12*(3), 355.
7. Hossain, M. S., Bujang, J. S., Zakaria, M. H., & Hashim, M. (2015). The application of remote sensing to seagrass ecosystems: an overview and future research prospects. *International Journal of Remote Sensing*, *36*(1), 61–114.

8. Islam, K. A. (2021). *Deep Learning Approaches for Seagrass Detection in Multispectral Imagery*. Old Dominion University.
9. Kaufman, K. A., & Bell, S. S. (2022). The use of imagery and GIS techniques to evaluate and compare seagrass dynamics across multiple spatial and temporal scales. *Estuaries and Coasts*, *45*(4), 1028–1044.
10. Koedsin, W., Intararuang, W., Ritchie, R. J., & Huete, A. (2016). An integrated field and remote sensing method for mapping seagrass species, cover, and biomass in southern Thailand. *Remote Sensing*, *8*(4), 292.
11. Komatsu, T., Hashim, M., Nurdin, N., Noiraksar, T., Prathep, A., Stankovic, M., & Hayashizaki, K. (2020). Practical mapping methods of seagrass beds by satellite remote sensing and ground truthing. *Coastal Marine Science*, *43*(1), 1–25.
12. Kovacs, E., Roelfsema, C., Lyons, M., Zhao, S., & Phinn, S. (2018). Seagrass habitat mapping: how do Landsat 8 OLI, Sentinel-2, ZY-3A, and Worldview-3 perform? *Remote Sensing Letters*, *9*(7), 686–695.
13. Lyons, M. B., Roelfsema, C. M., & Phinn, S. R. (2013). Towards understanding temporal and spatial dynamics of seagrass landscapes using time-series remote sensing. *Estuarine, Coastal and Shelf Science*, *120*, 42–53.
14. Maheswari, R. U. (2013). Mapping the under water habitat related to their bathymetry using Worldview-2 (wv-2) coastal, yellow, rededge, nir-2 satellite imagery in Gulf of Mannar to conserve the marine resource. *International Journal of Marine Science*, *3*(11).
15. McKenzie, L. J., Langlois, L. A., & Roelfsema, C. M. (2022). Improving approaches to mapping seagrass within the great barrier reef: from field to spaceborne earth observation. *Remote Sensing*, *14*(11), 2604.
16. Mohamed, H., Nadaoka, K., & Nakamura, T. (2020). Semiautomated mapping of benthic habitats and seagrass species using a convolutional neural network framework in shallow water environments. *Remote Sensing*, *12*(23), 4002.
17. O'Neill, J. D., Costa, M., & Sharma, T. (2011). Remote sensing of shallow coastal benthic substrates: in situ spectra and mapping of eelgrass (Zostera marina) in the Gulf Islands National Park Reserve of Canada. *Remote Sensing*, *3*(5), 975–1005.
18. Parthasarathy, N., Ravikumar, K., Ganesan, R., & Ramamurthy, K. (1991). Distribution of seagrasses along the coast of Tamil Nadu, Southern India. *Aquatic Botany*, *40*(2), 145–153.

19. Pasqualini, V., Pergent-Martini, C., Clabaut, P., Marteel, H., & Pergent, G. (2001). Integration of aerial remote sensing, photogrammetry, and GIS technologies in seagrass mapping. *Photogrammetric Engineering and Remote Sensing*, *67*(1), 99–105.
20. Paulose, N. E., Dilipan, E., & Thangaradjou, T. (2013). Integrating Indian remote sensing multi-spectral satellite and field data to estimate seagrass cover change in the Andaman and Nicobar Islands, India. *Ocean Science Journal*, *48*(2), 173–181.
21. Phinn, S., Roelfsema, C., Dekker, A., Brando, V., & Anstee, J. (2008). Mapping seagrass species, cover and biomass in shallow waters: An assessment of satellite multi-spectral and airborne hyper-spectral imaging systems in Moreton Bay (Australia). *Remote Sensing of Environment*, *112*(8), 3413–3425.
22. Phiri, D., Simwanda, M., Salekin, S., Nyirenda, V. R., Murayama, Y., & Ranagalage, M. (2020). Sentinel-2 data for land cover/use mapping: A review. *Remote Sensing*, *12*(14), 2291.
23. Pu, R., Bell, S., Baggett, L., Meyer, C., & Zhao, Y. (2012). Discrimination of seagrass species and cover classes with in situ hyperspectral data. *Journal of Coastal Research*, *28*(6), 1330–1344.
24. Roelfsema, C. M., Lyons, M., Kovacs, E. M., Maxwell, P., Saunders, M. I., Samper-Villarreal, J., & Phinn, S. R. (2014). Multi-temporal mapping of seagrass cover, species and biomass: A semi-automated object based image analysis approach. *Remote Sensing of Environment*, *150*, 172–187.
25. Roelfsema, C. M., Phinn, S. R., & Joyce, K. (2016). *Spectral reflectance library of algal, seagrass and substrate types in Moreton Bay, Australia [dataset]*. PANGAEA. https://doi.org/10.1594/PANGAEA.864310
26. Roelfsema, C. M., Phinn, S. R., Udy, N., & Maxwell, P. (2009). An integrated field and remote sensing approach for mapping seagrass cover, Moreton Bay, Australia. *Journal of Spatial Science*, *54*(1), 45–62.
27. Strydom, S., Webster, C. L., McCallum, R., Lafratta, A., O'Dea, C. M., Said, N. E., Inostroza, K., Salinas, C., Billinghurst, S., Phelps, C. M., Campbell, C., Gorham, C., Dunham, N., Bernasconi, R., Frouws, A. M., Werner, A., Vitelli, F., Puigcorbé, V., D'Cruz, A., … Serrano, Ó. (2021). *Global database of key seagrass structure, biomass and production variables [dataset]*. PANGAEA. https://doi.org/10.1594/PANGAEA.929968
28. Vahtmäe, E., Argus, L., Toming, K., Ligi, M., & Kutser, T. (2024). *Reflectance spectra of submerged aquatic vegetation (SAV) species and substrates from the Baltic Sea coastal waters [dataset]*. PANGAEA. https://doi.org/10.1594/PANGAEA.971518